

# Optimal efficiency of quantum transport in a disordered trimer

Giulio G. Giusteri,<sup>1,2,\*</sup> G. Luca Celardo,<sup>2</sup> and Fausto Borgonovi<sup>2</sup>

<sup>1</sup>*Mathematical Soft Matter Unit, Okinawa Institute of Science and Technology Graduate University, 1919-1 Tancha, Onna-son, Kunigami-gun, Okinawa, Japan 904-0495*

<sup>2</sup>*Dipartimento di Matematica e Fisica and Interdisciplinary Laboratories for Advanced Materials Physics, Università Cattolica del Sacro Cuore, via Musei 41, I-25121 Brescia, Italy  
and Istituto Nazionale di Fisica Nucleare, Sezione di Pavia, via Bassi 6, I-27100, Pavia, Italy*  
(Dated: March 7, 2022)

Disordered quantum networks, as those describing light-harvesting complexes, are often characterized by the presence of peripheral ring-like structures, where the excitation is initialized, and inner structures, reaction centers (RC), where the excitation is trapped and transferred. The peripheral rings often display distinguished coherent features: their eigenstates can be separated, with respect to the transfer of excitation, in the two classes of superradiant and subradiant states. Both are important to optimize transfer efficiency. In the absence of disorder, superradiant states have an enhanced coupling strength to the RC, while the subradiant ones are basically decoupled from it. Static on-site disorder induces a coupling between subradiant and superradiant states, thus creating an indirect coupling to the RC. The problem of finding the optimal transfer conditions, as a function of both the RC energy and the disorder strength, is very complex even in the simplest network, namely a three-level system. In this paper we analyze such trimeric structure choosing as initial condition an excitation on a subradiant state, rather than the more common choice of an excitation localized on a single site. We show that, while the optimal disorder is of the order of the superradiant coupling, the optimal detuning between the initial state and the RC energy strongly depends on system parameters: when the superradiant coupling is much larger than the energy gap between the superradiant and the subradiant levels, optimal transfer occurs if the RC energy is at resonance with the subradiant initial state, whereas we find an optimal RC energy at resonance with a virtual dressed state when the superradiant coupling is smaller than or comparable with the gap. The presence of dynamical noise, which induces dephasing and decoherence, affects the resonance structure of energy transfer producing an additional “incoherent” resonance peak, which corresponds to the RC energy being equal to the energy of the superradiant state.

PACS numbers: 05.60.Gg, 71.35.-y

## I. INTRODUCTION

Photosynthetic bacteria utilize antenna complexes to capture photons and convert the energy of the short-lived electronic excitation in a more stable form, such as chemical bonds. After absorption, the energy is transferred to a complex, called reaction center (RC), where it initiates electron transfer, resulting in a membrane potential. This very efficient transfer occurs on a time-scale of few hundreds of picoseconds and on a length-scale of few nanometers, so that coherent quantum dynamics can enter the play, as recent experiments seem to prove [1]. Quantum coherence can enhance transport efficiency inducing Supertransfer and Superradiance in light-harvesting complexes [2–4]. On the other hand, quantum coherence can also be detrimental to transport, as Anderson localization [5] and the presence of trapping-free subspaces [6] show.

Superradiance [7–9], as viewed in the context of both optical fluorescence [10–12] and quantum transport in open systems [2, 13–16], is not solely a many-body effect. Single-excitation superradiance is a prominent example

of genuinely quantum cooperative effect [17], relevant in natural complexes, which operate in the single excitation regime since solar light is very dilute.

Natural complexes are subject to a noisy environment with different correlation time-scales (if compared to the excitonic transport time): (i) short-time correlations, giving rise to dephasing (homogeneous broadening, as considered e.g. in [18–21]) and (ii) long-time correlations, producing on-site static disorder (inhomogeneous broadening, as considered e.g. in [22, 23]). Following a common nomenclature, we will refer to the former effect as dephasing noise and to the latter as static disorder.

The role of environment is twofold: on one hand, it can help transport since it destroys the detrimental coherent effects, leading to noise-enhanced energy transfer, i.e. the existence of a maximal efficiency at some intermediate noise strength, as found in the last decade by various groups [6, 18–21, 24–30]. On the other hand, it can suppress the beneficial coherences leading to a quenching of Supertransfer [15]. It is thus essential to consider this non-trivial interplay.

Typical structures of bacterial photosynthetic complexes display a RC placed at the center of the light-harvesting complex I (LHI), with the chromophores arranged on a ring and surrounded by other ring structures (called LHII) acting as peripheral antennae. The LHI-RC

\* giulio.giusteri@oist.jp

structure describing light-harvesting complexes produces a distinguished feature: the eigenstates of the peripheral ring structure can be separated into two classes, superradiant and subradiant states, with respect to the transfer of excitation towards the RC. In absence of both environmental noise and static disorder, the superradiant states are coupled to the RC with a coupling amplitude proportional to  $\sqrt{N}$ , where  $N$  is the number of chromophores in the ring, while subradiant states are basically decoupled from the RC. In presence of disorder, the subradiant states can be coupled to the superradiant ones and, as a consequence, only indirectly coupled to the RC states. Note that the subradiant subspace, previously studied by the authors [15], has been also analyzed in the literature under the name of trapping-free subspace [6].

The optimization of excitation transfer efficiency from peripheral states in networks displaying the Ring-RC structure is a rather difficult problem, even for a network as simple as a trimer. Despite its simplicity, the trimer model has been discussed in several papers as a paradigmatic model [18, 31]. In particular, in [18] various optimal conditions are explored in simple few-site networks in the presence of dephasing noise but without static disorder. Since it is difficult to clarify generic physical effects by studying specific natural systems, we rather investigate the simplest model for quantum transport that displays the features mentioned above: a disordered trimer with a superradiant and a subradiant state, on which the excitation is initialized, along with an acceptor state (the RC), where the excitation can be trapped, see Fig. 1a. We believe this to be an essential step towards understanding the basic mechanism of transfer optimization in more complex networks.

Here we discuss the optimization of excitation transfer efficiency when the excitation is initially prepared on a subradiant state rather than on a single site, as is usually done. There are two main reasons for considering transport from a subradiant initial condition, related to the presence of noise and disorder: (i) The thermalization processes, typically at place in natural complexes, such as the LHI-RC of purple bacteria, tend to populate the lowest-energy levels, which include both superradiant and subradiant states with respect to the RC and to the electromagnetic field [15, 32]. (ii) In absence of any noise, subradiant states do not contribute to transport efficiency. The presence of moderate static disorder hinders super- and sub-radiance, causing subradiant states to become significantly open to transport. Hence, a moderate disorder increases the transport efficiency of subradiant states. At the same time, a very large disorder ultimately prevents transport, due to Anderson localization. Since disorder is only detrimental for superradiant states, the overall optimization of transfer is determined by the behavior of subradiant states.

To pursue our goal, in Section II we present our trimer model. In Fig. 1b, the trimer is shown in the super-subradiant basis to stress the following features: in the absence of disorder, while the subradiant state is decou-

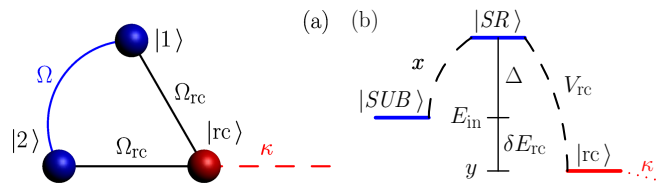


FIG. 1. (Color online) In panel (a) the trimer model is shown in the site basis: two sites connected with the RC with equal coupling  $\Omega_{rc}$  and between them with coupling  $\Omega$ . In panel (b) the trimer model is shown in the superradiant-subradiant-RC basis, see text.

pled from the RC, the superradiant state has an enhanced coupling  $V_{rc}$  to the RC. We discuss the maximization of the average (over disorder) transfer efficiency with respect to both the detuning  $\delta E_{rc}$  between initial subradiant state and RC and the strength  $W$  of disorder. We have found two different regimes depending on  $V_{rc}$  and the energy gap  $\Delta$  between the subradiant and superradiant states. The optimal detuning is achieved when the energy of the RC is at resonance with the initial state (subradiant) for  $V_{rc} \gg \Delta$ , while we have found a less trivial optimal detuning, namely  $\delta E_{rc} = V_{rc}^2/\Delta$ , in the case  $V_{rc} \leq \Delta$ . This can be interpreted as a resonant condition between dressed states. Concerning the optimal disorder, we have found that it is always of the order of  $V_{rc}$ , if  $V_{rc}$  is larger or comparable with  $\Delta$ , while it is smaller when  $V_{rc} \ll \Delta$ .

We analyze in Section III how our findings are affected by dephasing. Since our aim is to analyze in detail a very simplified model, we include in a paradigmatic way the effects of a dephasing environment, adopting the Haken-Strobl model [33]. Such an effective master equation assumes white-noise fluctuations of the site energies, thereby implying a high-temperature limit. Even if it is possible to consider more refined phononic baths, they are not necessary here due to the simplicity of our model. Moreover, they have been found to give results that are qualitatively similar to those obtained with the Haken-Strobl approach [2–4].

We show that dynamical noise induces an additional resonance peak when the RC energy is equal to the energy of the superradiant state. Indeed, the incoherent path opened by dephasing favours transport between those states which are directly coupled, making the final hopping between the superradiant state and the RC the key passage of the transport process. By contrast, the coherent resonance condition found in the absence of dephasing takes into account the interference effects which are present in the system as a whole, emphasizing the role of the initial condition in determining the transport efficiency.

## II. THE DISORDERED TRIMER MODEL

The Hamiltonian (in site-basis) for the trimer model depicted in Fig. 1a can be written in matrix form as follows:

$$\begin{pmatrix} E_1 - i\frac{\Gamma_{\text{fl}}}{2} & \Omega & \Omega_{\text{rc}} \\ \Omega & E_2 - i\frac{\Gamma_{\text{fl}}}{2} & \Omega_{\text{rc}} \\ \Omega_{\text{rc}} & \Omega_{\text{rc}} & E_{\text{rc}} - i\frac{\Gamma_{\text{fl}} + \kappa}{2} \end{pmatrix}, \quad (1)$$

where the action of the environment (static disorder) has been taken into account by choosing the energy levels  $E_k$ ,  $k = 1, 2$ , as Gaussian random numbers with mean zero and variance  $W^2$ , and no disorder has been added to the RC site (its effect can be naturally embedded as additional disorder on the sites 1 and 2).

The loss of excitation through the RC has been described by the non-Hermitian term  $-i\kappa/2$ . Throughout the whole paper,  $\kappa$  is assumed to be small with respect to the other coupling parameters. This choice is consistent with the realistic photosynthetic models. In order to make a close comparison with realistic systems and following a standard procedure [2, 3, 14–16], we also introduced the diagonal non-Hermitian terms  $-i\Gamma_{\text{fl}}/2$ , with the fluorescence constant  $\Gamma_{\text{fl}}$  much smaller than any other energy scale ( $\Omega, \Omega_{\text{rc}}, W, \kappa$ ), representing the loss of excitation from each site due to recombination.

It is convenient to move from the site-basis to the subradiant-superradiant-RC basis by defining the states

$$|SUB\rangle = \frac{1}{\sqrt{2}}(|1\rangle - |2\rangle),$$

$$|SR\rangle = \frac{1}{\sqrt{2}}(|1\rangle + |2\rangle),$$

from which the new Hamiltonian  $H$  easily follows (see also Fig. 1b):

$$H = \begin{pmatrix} -\Omega - i\frac{\Gamma_{\text{fl}}}{2} & x & 0 \\ x & \Omega - i\Gamma_{\text{fl}}/2 & \sqrt{2}\Omega_{\text{rc}} \\ 0 & \sqrt{2}\Omega_{\text{rc}} & y - i\frac{\Gamma_{\text{fl}} + \kappa}{2} \end{pmatrix}, \quad (2)$$

where the two Gaussian random variables  $x = (E_1 - E_2)/2$  and  $y = E_{\text{rc}} - (E_1 + E_2)/2$  are such that  $\langle x \rangle = 0$ ,  $\langle y \rangle = E_{\text{rc}}$ , and  $\langle x^2 \rangle = \langle y^2 \rangle - E_{\text{rc}}^2 = W^2/2$ .

In this basis, the coupling between the subradiant state and the RC vanishes, whereas the coupling between the superradiant state and the RC is enhanced and it is given by the matrix element  $V_{\text{rc}} = \sqrt{2}\Omega_{\text{rc}}$ . The structure of the Hamiltonian, depicted in Fig. 1b, implies that the excitation transfer from the subradiant state to the RC can only be mediated by the superradiant state, through the random coupling  $x$ . In this basis, the trimer model subradiant-superradiant-RC corresponds to a donor-bridge-acceptor (DBA) system without direct

coupling between the donor and the acceptor and with a random coupling between donor and bridge and a random acceptor energy. In spite of the fact that similar systems have been widely studied in literature, the analysis developed in the present article concerning the optimization of the decay of an excitation, initialized on the donor state and dissipated at the level of the acceptor state, with the stochastic terms considered here, appears to be new, to the best of our knowledge. More importantly, our analysis lies outside the regime of validity of perturbation theory, which is used within the superexchange mechanism [34] to study these systems. Indeed, the superexchange mechanism can be applied only when the donor-bridge coupling is much smaller than the donor-bridge energy detuning (in our case this detuning can be even zero).

A most important quantity for such an analysis (motivated by the study of light-harvesting complexes but also relevant in a general context) is the efficiency, at the time  $t$ , of energy transfer from the system into the RC. Given an initial state  $|\Psi_{\text{in}}\rangle$ , it is defined as [19, 20]

$$\eta_{\Psi_{\text{in}}}(t) = \left\langle \kappa \int_0^t |\langle \text{RC} | e^{-\frac{i}{\hbar} H \tau} | \Psi_{\text{in}} \rangle|^2 d\tau \right\rangle_W, \quad (3)$$

and it represents the probability of escaping out of the system up to the time  $t$ . In the above definition the brackets  $\langle \dots \rangle_W$  indicate the average over disorder.

In numerical simulations we always consider the efficiency at a time  $t \gtrsim \hbar/\Gamma_{\text{fl}}$ . Note that the efficiency strongly depends on the time  $t$  at which it is computed for  $t < \hbar/\Gamma_{\text{fl}}$ , while it reaches a stable asymptotic value  $\eta^\infty$  for  $t \gtrsim \hbar/\Gamma_{\text{fl}}$ , thus motivating our choice. As  $\Gamma_{\text{fl}} \rightarrow 0$ , the asymptotic value of the efficiency is  $\eta^\infty = 1$  for any choice of parameters. According to a common practice in the study of light-harvesting systems, we will measure energies in  $\text{cm}^{-1}$  and times in ps.

It is clear from (3) that the energy transfer efficiency is strongly dependent upon the initial state, a feature also studied in [23]. Indeed, if we start from the superradiant state we are in a situation in which there is an enhanced direct coupling to the RC at zero disorder. Thus, one might think that the best situation occurs when the excitation is on the superradiant state set at resonance with the energy of the RC. In this situation disorder is only detrimental to transport, since it tends to destroy the superradiant coupling [10, 15] and it moves the system out of resonance. On the other side, the excitation in natural complexes is usually spread also on subradiant states, due to the presence of a thermal bath. Since a subradiant state is not directly coupled to the RC, it is only through the action of disorder that the excitation can be transferred from the initial state to the RC (i.e. for  $W = 0$ , we have  $\eta = 0$ ).

We will focus our attention on this non-trivial case (see Fig. 1b), in which an initial excitation is on the subradiant state at energy  $E_{\text{in}} = -\Omega$ , coupled via  $x$  to the superradiant state at energy  $E_{\text{sr}} = \Omega = E_{\text{in}} + \Delta$ , which is further coupled to the RC with the tunnelling amplitude

$V_{\text{rc}} = \sqrt{2}\Omega_{\text{rc}}$ . Our aim is to find the system configuration that maximizes the average transfer efficiency. Fixing the energy gap  $\Delta = 2\Omega$  between the superradiant and the subradiant states and the superradiant-RC coupling  $V_{\text{rc}}$ , and assuming  $\kappa$  and  $\Gamma_{\text{fl}}$  to be perturbative quantities, we are left with two independent parameters to be tuned to achieve the maximal efficiency: the subradiant-RC detuning  $\delta E_{\text{rc}} = E_{\text{rc}} - E_{\text{in}}$  and the strength  $W$  of the random coupling  $x$ .

To pursue our goal we will first analyze a fully deterministic model obtained replacing the stochastic terms  $x$  and  $y$  in equation (2) with deterministic parameters  $X$  and  $E_{\text{rc}}$  as follows:

$$H^{\text{det}} = \begin{pmatrix} E_{\text{in}} - i\frac{\Gamma_{\text{fl}}}{2} & X & 0 \\ X & E_{\text{in}} + \Delta - i\frac{\Gamma_{\text{fl}}}{2} & V_{\text{rc}} \\ 0 & V_{\text{rc}} & E_{\text{rc}} - i\frac{\Gamma_{\text{fl}} + \kappa}{2} \end{pmatrix}. \quad (4)$$

In what follows, we analyze the results of the deterministic model comparing them with the results in presence of disorder. In figures 2, 4, and 5 the results of the deterministic model are shown in the left panels, while those in presence of disorder, are in the right panels.

### A. Optimal disorder and resonance conditions

According to our previous assumptions, the behavior of the efficiency  $\eta$  in both the  $(X, \delta E_{\text{rc}})$  and  $(W, \delta E_{\text{rc}})$  planes depends on the ratio between the two system parameters  $\Delta$  and  $V_{\text{rc}}$ . We first consider the case  $\Delta = 0$ , which corresponds to two uncoupled sites in the trimer model ( $\Omega = 0$ ) equally connected to the RC. In this case, the sole energy scale of the system is  $V_{\text{rc}}$ . We will subsequently consider the effects of a finite gap  $\Delta \neq 0$ .

We observe that in most of the regimes we consider here, where  $\Delta$  is very small compared to other parameters, we cannot rely on the superexchange interaction approach (very effective in other treatment of similar systems where a donor and an acceptor are not directly coupled, see for instance [34]) to find optimality conditions, since the perturbative assumptions used there are not generically valid in our context.

#### 1. The zero-gap case: $\Delta = 0$ .

With  $\Delta = 0$  our model corresponds to a tight-binding chain of three sites, the first (subradiant) is coupled via  $X$  to the second (superradiant), with equal energy, which is coupled to the RC with strength  $V_{\text{rc}}$ . It can be easily checked that, if we initially excite the subradiant state, the probability  $P_{\text{RC}}(t)$  of finding the excitation on the RC (which is a periodic function of time if we neglect the non-Hermitian terms in (4)) can reach the maximal value of 1 in the shortest time when  $X = V_{\text{rc}}$  and  $\delta E_{\text{rc}} = 0$ , thus

identifying the following global optimization condition:

$$X_{\text{opt}} = V_{\text{rc}} \quad \text{and} \quad \delta E_{\text{rc}}^{\text{opt}} = 0. \quad (5)$$

The estimate given in (5), obtained considering the coherent transfer of excitation between the subradiant and the RC states, is a very good estimate also of the global optimum of the transfer efficiency, as shown in Fig. 2 (blue cross in panel (a)). We observe that the condition  $\delta E_{\text{rc}} = 0$  is not necessary for the probability of being on the RC to reach 1, but, in combination with  $X = V_{\text{rc}}$ , it makes such transfer the fastest.

On the other hand, if we have some constraint on the coupling  $X$  enforcing the condition  $X \gg V_{\text{rc}}$ , the optimal detuning is not given by  $\delta E_{\text{rc}} = 0$ . To find the detuning producing the optimal transfer in the case  $X \gg V_{\text{rc}}$  we can consider  $V_{\text{rc}}$  as a perturbation, obtaining the picture illustrated in panel (a) of Fig. 3. The subradiant and superradiant states couple and give rise to the dressed energy levels

$$\varepsilon_{\pm}(X) = E_{\text{in}} + \frac{\Delta}{2} \pm \sqrt{\frac{\Delta^2}{4} + X^2}, \quad (6)$$

which reduce to  $\varepsilon_{\pm}(X) = E_{\text{in}} \pm X$  for  $\Delta = 0$  (recall that we considered both  $\kappa$  and  $\Gamma_{\text{fl}}$  as small perturbations, that can be neglected in finding the dressed energies). The initial excitation is equally distributed on those levels, and we can then identify two optimal detuning values by the symmetric resonant tunneling conditions

$$E_{\text{rc}} = \varepsilon_{\pm}(X), \quad (7)$$

entailing

$$\delta E_{\text{rc}}(X) = \frac{\Delta}{2} \pm \sqrt{\frac{\Delta^2}{4} + X^2}. \quad (8)$$

In our case, since  $\Delta = 0$ , we have  $\delta E_{\text{rc}}(X) = \pm X$  (see dashed curves in Fig. 2). Note that in (8) we kept the dependence on  $\Delta$ , since it will be relevant to what follows.

As can be clearly seen from Fig. 2, the results obtained from the deterministic model are in good agreement with those in presence of disorder. Indeed, we can obtain an excellent estimate for the global optimization condition by simply substituting the deterministic coupling  $X$  with  $W/\sqrt{2}$  in (5) (blue cross panel (b) of Fig. 2).

#### 2. The finite-gap case I: $V_{\text{rc}} \gg \Delta$ .

We now investigate whether the optimal conditions given in equation (5) are valid also for finite values of the energy gap  $\Delta$ .

Let us first consider the situation where  $\Delta < V_{\text{rc}}$ . We see from Fig. 4 that the global optimization condition (5) (blue cross) is still an excellent estimate for the configuration with maximal efficiency, and also the symmetric resonances present for  $X \gg V_{\text{rc}}$  follow the analytic prediction (8) (see dashed curves in Fig. 4). Nevertheless,



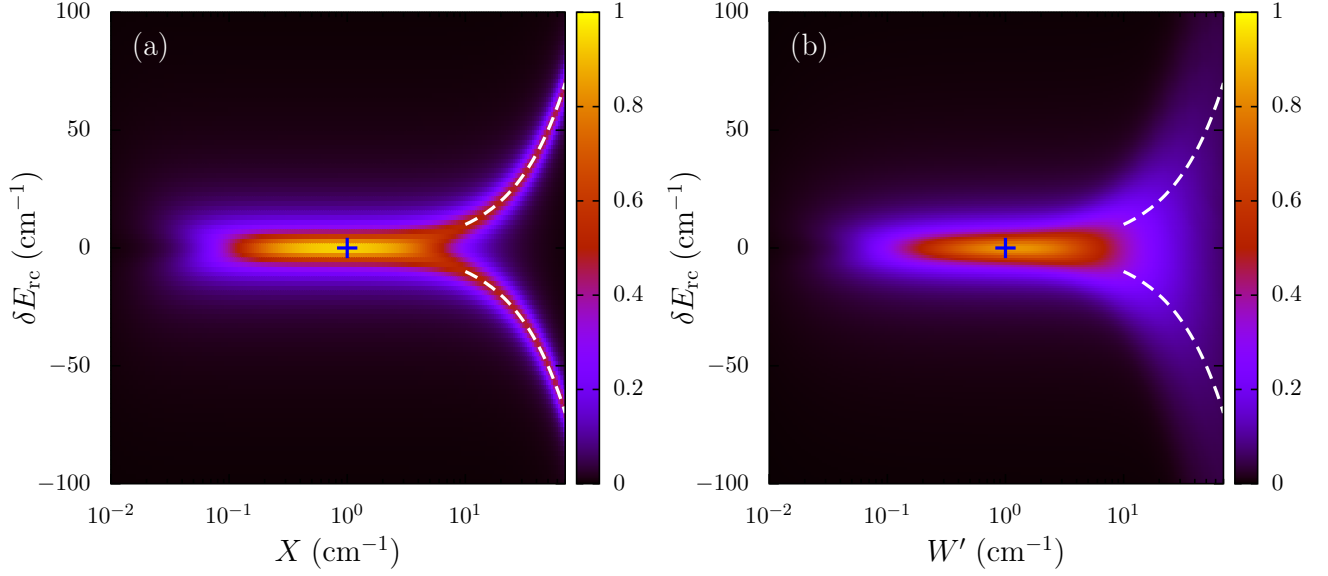


FIG. 2. (Color online) Average transfer efficiency  $\eta$ , computed starting from the subradiant state  $|SUB\rangle$ , plotted in panel (a) as a function of the subradiant-RC detuning  $\delta E_{rc}$  and of the deterministic subradiant-superradiant coupling  $X$ , and in panel (b) as a function of  $\delta E_{rc}$  and of the rescaled disorder strength  $W' = W/\sqrt{2}$ . The blue cross indicates the estimate (5) for the optimal transfer conditions. The dashed curves indicate the resonances determined in (8). The values of the parameters are  $\Delta = 0 \text{ cm}^{-1}$ ,  $V_{rc} = 1 \text{ cm}^{-1}$ ,  $\kappa = 0.01 \text{ cm}^{-1}$ , and  $\Gamma_{\text{fl}} = 10^{-4} \text{ cm}^{-1}$ . We sampled the efficiency on a  $100 \times 100$  uniform grid in panel (a) and on a  $100 \times 200$  uniform grid in panel (b), where the ensemble average over 2000 realizations of static disorder is shown.

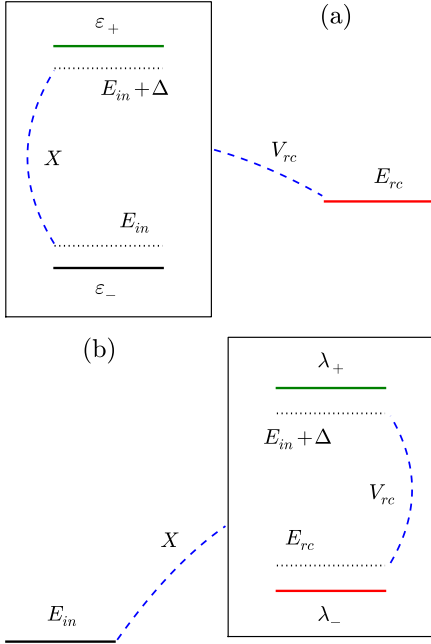


FIG. 3. (Color online) Different schematic representations of the energy levels in the deterministic trimer model. (a) The subradiant-superradiant subsystem (framed), where the coupling  $X$  produces the dressed levels with energies  $\varepsilon_{\pm}$ , is coupled through  $V_{rc}$  to the RC state at energy  $E_{rc}$ . (b) The initial subradiant state at energy  $E_{in}$  is coupled through  $X$  to the superradiant-RC subsystem (framed), where the coupling  $V_{rc}$  produces the dressed levels with energies  $\lambda_{\pm}$ .

Fig. 4 enlightens a somewhat unexpected feature: if we assume now the coupling  $X$  to be constrained within the region  $X \ll \Delta < V_{rc}$ , the RC energy producing the maximal efficiency, identified by a sharp resonance, is very far from either  $E_{in}$  or  $\varepsilon_{\pm}$ .

To understand such a resonance, we can now consider  $X$  as a small perturbation, exploiting the picture illustrated in panel (b) of Fig. 3. The superradiant and the RC states couple to give the dressed energy levels

$$\lambda_{\pm}(E_{rc}) = \frac{E_{in} + \Delta + E_{rc}}{2} \pm \sqrt{\frac{(E_{in} + \Delta - E_{rc})^2}{4} + V_{rc}^2}, \quad (9)$$

which clearly depend on the RC energy  $E_{rc}$ . The initial excitation is all on the subradiant state, since  $X$  is small, and a resonant tunneling criterion would now require  $E_{in}$  to match the energies  $\lambda_{\pm}$  of the superradiant-RC subsystem. Nevertheless, we have  $E_{in} < E_{in} + \Delta < \lambda_{+}$  by construction, so that the resonant condition for  $X \ll \Delta < V_{rc}$  must be

$$E_{in} = \lambda_{-}(E_{rc}), \quad (10)$$

entailing

$$\delta E_{rc} = \frac{V_{rc}^2}{\Delta}, \quad (11)$$

which matches exactly the numerical results (see dot-dashed line in Fig. 4).

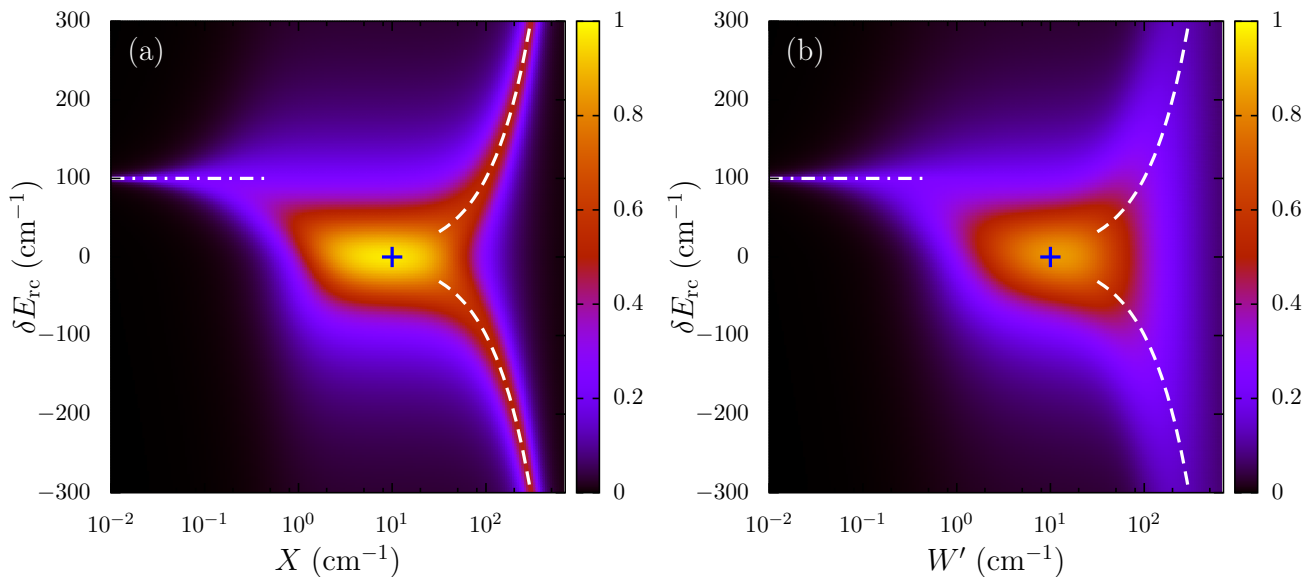


FIG. 4. (Color online) Average transfer efficiency  $\eta$ , computed starting from the subradiant state  $|SUB\rangle$ , plotted in panel (a) as a function of the subradiant-RC detuning  $\delta E_{rc}$  and of the deterministic subradiant-superradiant coupling  $X$ , and in panel (b) as a function of  $\delta E_{rc}$  and of the rescaled disorder strength  $W' = W/\sqrt{2}$ . The blue cross indicates the estimate (5) for the optimal transfer conditions. The dashed curves indicate the resonances determined in (8) and the dot-dashed line marks the the resonant condition (11). The values of the parameters are  $\Delta = 1 \text{ cm}^{-1}$ ,  $V_{rc} = 10 \text{ cm}^{-1}$ ,  $\kappa = 0.01 \text{ cm}^{-1}$ , and  $\Gamma_{fl} = 10^{-4} \text{ cm}^{-1}$ . We sampled the efficiency on a  $100 \times 300$  uniform grid in both panels. In panel (b) the ensemble average over 2000 realizations of static disorder is shown.

Concerning the model in presence of disorder, we can again obtain an excellent estimate for the global optimization condition by simply substituting the deterministic coupling  $X$  with  $W/\sqrt{2}$  in (5) (blue cross in panel (b) of Fig. 4).

### 3. The finite-gap case II: $V_{rc} \lesssim \Delta$ .

If we now decrease further the ratio  $V_{rc}/\Delta$  we find the following remarkable result (panel (a) of Fig. 5): the estimate (5), which was obtained for  $V_{rc} \gg \Delta$ , still identifies the global efficiency optimization in the deterministic model (blue cross). Moreover, the resonances predicted by (8) for  $X \gg V_{rc}, \Delta$  and by (11) for  $X \ll V_{rc}, \Delta$  still correspond to the local optimization of the efficiency (see white curves in Fig. 5). As for the model in presence of disorder (panel (b) of Fig. 5), while the estimate (5) is still within a region of significant efficiency, the optimal condition is modified by disorder, (see panels (c) and (d) of Fig. 5 and the discussion below).

Indeed, when  $V_{rc} \lesssim \Delta$  (Figure 5), disorder induces some modification of the global optimization conditions. This effect can be clearly seen by comparing panels (c) and (d) of Fig. 5, which describe a situation with  $V_{rc}/\Delta \approx 0.5$ . The average over disorder shifts the optimal detuning from  $\delta E_{rc} = 0$  to the low-disorder resonance  $\delta E_{rc} = V_{rc}^2/\Delta$  given by (11). This can be explained by the fact that the random coupling falls for many realizations in the region  $X < V_{rc} \lesssim \Delta$ , where the resonance

is for  $\delta E_{rc} = V_{rc}^2/\Delta$  and not for  $\delta E_{rc} = 0$ . As far as optimal disorder is concerned, even if (5) overestimates its actual value, it still gives an estimate within 5% of the maximal efficiency (panel (d) of Fig. 5). In general for  $V_{rc} \ll \Delta$  we have verified that the optimal detuning is still given by  $\delta E_{rc} = V_{rc}^2/\Delta$ , while the optimal disorder shifts towards zero as  $V_{rc}$  decreases. This is again an effect of the average over disorder realizations, due to the fact that the resonance condition  $\delta E_{rc} = V_{rc}^2/\Delta$  is valid for small disorder.

### B. Summary for the case with only static disorder

Summarizing, the global optimization of the average transfer efficiency  $\eta(t \gtrsim \hbar/\Gamma_{fl})$  from the subradiant state of the trimer into the sink placed at the RC is given by

$$W_{opt}/\sqrt{2} \simeq V_{rc} \quad \text{and} \quad E_{rc} = E_{in} \quad \text{for} \quad V_{rc} \gg \Delta, \quad (12)$$

and

$$W_{opt}/\sqrt{2} \simeq V_{rc} \quad \text{and} \quad E_{rc} = E_{in} + \frac{V_{rc}^2}{\Delta} \quad \text{for} \quad V_{rc} \lesssim \Delta. \quad (13)$$

Another physically relevant question concerns the optimal detuning at some fixed disorder strength determined by physiological conditions (natural systems are usually subject to a definite range of static disorder). In this situation our results indicate that, if the disorder is constrained to be smaller than the energy gap  $\Delta$  and the

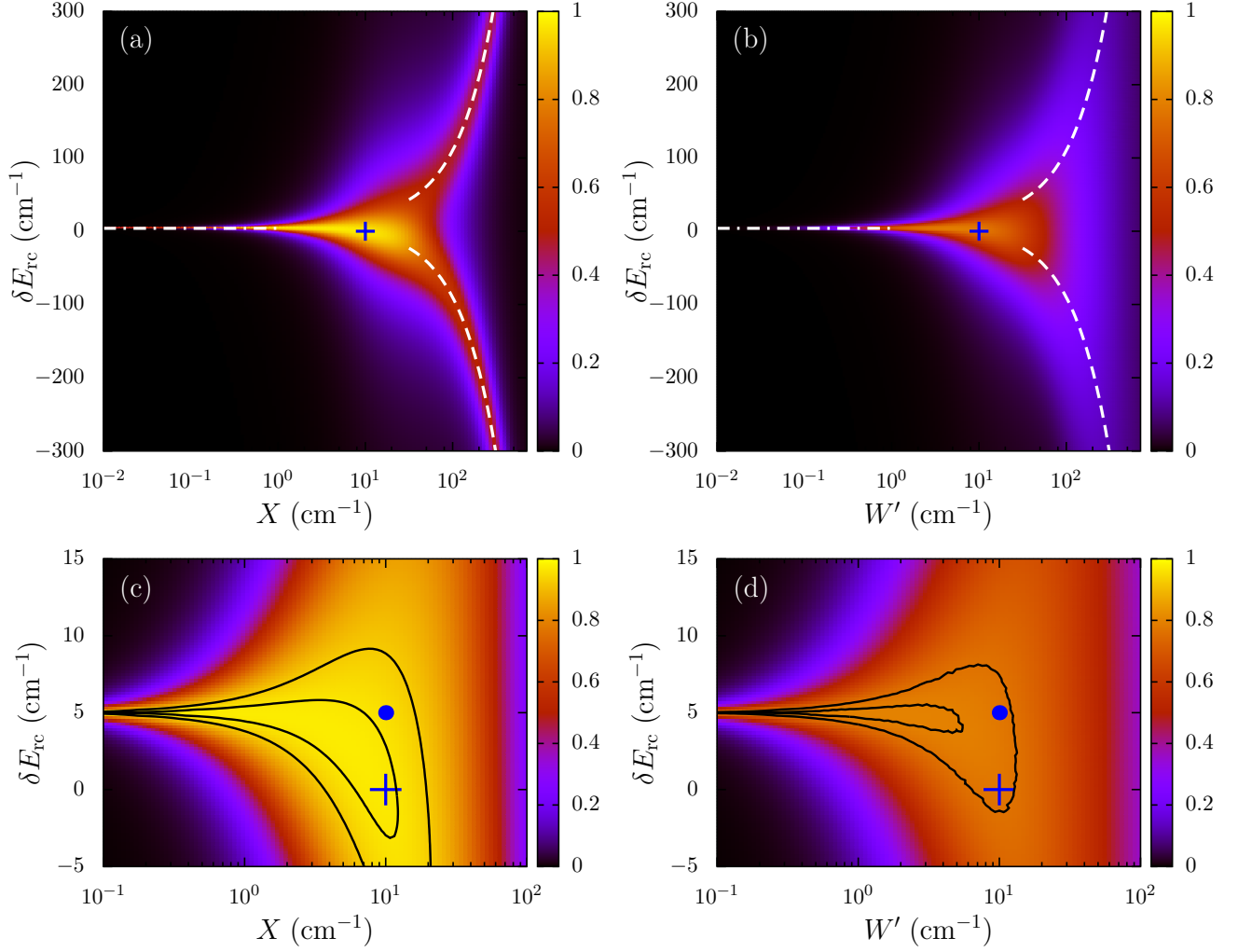


FIG. 5. (Color online) Average transfer efficiency  $\eta$ , computed starting from the subradiant state  $|SUB\rangle$ , plotted in panels (a) and (c) as a function of the subradiant-RC detuning  $\delta E_{rc}$  and of the deterministic subradiant-superradiant coupling  $X$ , and in panels (b) and (d) as a function of  $\delta E_{rc}$  and of the rescaled disorder strength  $W' = W/\sqrt{2}$ . The blue cross indicates the estimate (5) for the optimal transfer conditions. In panels (a) and (b) the dashed curves indicate the resonances determined in (8) and the dot-dashed line marks the the resonant condition (11). In panels (c) and (d) we zoomed on the high-efficiency regions to show how disorder affects the accuracy of the estimates (5) and (12). The blue dots mark the modification (13) of the estimate proposed in section II A 3. Isolines enclose the regions of efficiency lying within 1% and 5% of the maximal efficiency. The values of the parameters are  $\Delta = 20 \text{ cm}^{-1}$ ,  $V_{rc} = 10 \text{ cm}^{-1}$ ,  $\kappa = 0.01 \text{ cm}^{-1}$ , and  $\Gamma_{fl} = 10^{-4} \text{ cm}^{-1}$ . We sampled the efficiency on a  $100 \times 600$  uniform grid in panels (a) and (b) and on a  $60 \times 100$  uniform grid in panels (c) and (d). In panels (b) and (d) the ensemble average over 2000 realizations of static disorder is shown.

coupling  $V_{rc}$ , the optimal subradiant-RC detuning is not zero, but it is always given by

$$\delta E_{rc} = \frac{V_{rc}^2}{\Delta}, \quad (14)$$

with a significant efficiency present only in a narrow band around such optimal detuning. This result is at variance with the intuitive expectation that the best transport would be obtained at resonance with the initial state,  $\delta E_{rc} = 0$ .

For large values of the static disorder, as a result of the averaging procedure, we have a broad resonance cen-

tered around  $\delta E_{rc} = 0$ , which fades into two very broad resonances centered around  $E_{rc} = \varepsilon_{\pm}(W/\sqrt{2})$  given by condition (7), characterized by a negligible efficiency.

### III. THE EFFECT OF DEPHASING NOISE

We now discuss how the presence of dynamical noise affects the coherent features analyzed in the previous section. The coupling to a dephasing environment is modeled as stochastic fluctuations of diagonal energies, by adding to the Hamiltonian of the system the time-

dependent term

$$H_{\text{deph}} = \hbar \sum_{k=1}^3 q_k(t) |k\rangle \langle k|,$$

where the frequencies  $q_k(t)$  represent uncorrelated fluctuations characterized by

$$\langle q_k(t) q_{k'}(t') \rangle = \frac{\gamma_\phi}{\hbar} \delta_{kk'} \delta(t - t'), \quad (15)$$

with  $\gamma_\phi/\hbar$  being the dephasing rate. For the sake of comparison with the other system parameters, we represent the intensity of dephasing by the energy parameter  $\gamma_\phi$ .

This is a common way to include dephasing in excitation dynamics, and it gives rise to the Haken–Strobl master equation [33]. The Haken–Strobl approach has been widely used in the past to include dephasing [10, 35] and it has also been analyzed in many recent applications [16, 18–21, 24–30] for its simplicity and effectiveness in describing strong dephasing in the high-temperature limit.

Within this approach, it is possible to analytically perform the average over white noise and then consider the evolution of our trimer system as dictated by the following master equation for the average density matrix  $\rho$  ( $h, k = 1, 2, 3$  with  $3 = \text{RC}$ ):

$$\frac{d\rho_{hk}}{dt} = -\frac{i}{\hbar} (H\rho - \rho H^\dagger)_{hk} - \frac{\gamma_\phi}{\hbar} (1 - \delta_{hk}) \rho_{hk}, \quad (16)$$

where  $H$  is the non-Hermitian trimer Hamiltonian introduced in (1), which contains the time-independent random energies describing static disorder.

From the practical point of view, due to the low dimensionality of our model system, we can adopt a very effective computational strategy. Since Eq. (16) is a first-order linear differential equation for the average density matrix  $\rho$  governed by a symmetric super-operator, we can diagonalize the latter and then use the exponential map to obtain, with great accuracy, the time-evolution of  $\rho$  averaged over dynamical noise. We do this for each realization of static disorder, performing eventually the ensemble average. We can then say that the average over dynamical noise is treated analytically, while the average over static disorder is performed numerically.

The transfer efficiency, which depends upon the initial density matrix  $\rho^{\text{in}}$ , is now given by

$$\eta_{\rho^{\text{in}}}(t) = \left\langle \kappa \int_0^t \rho_{33}(\tau) d\tau \right\rangle_W. \quad (17)$$

where  $\langle \dots \rangle_W$  represents the average over static disorder.

As before, we study the efficiency at the fluorescence time  $t_{\text{fl}} = \hbar/\Gamma_{\text{fl}}$ . It is indeed clear that this is an important time-scale for the system, since most of the excitation goes away within  $t_{\text{fl}}$ . Consequently, if the dephasing  $\gamma_\phi$  is smaller than the fluorescence width  $\Gamma_{\text{fl}}$ , it will not have enough time to significantly affect the system dynamics. On the other hand, when  $\gamma_\phi > \Gamma_{\text{fl}}$ , the dephasing will affect the various coherent features of the dynamics within the trimer, as we discuss below.

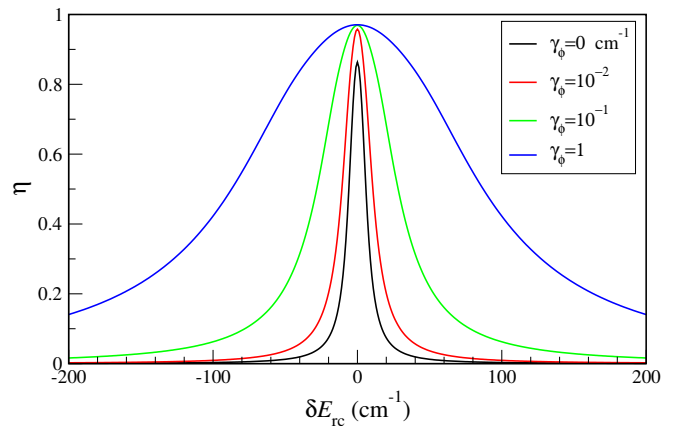


FIG. 6. (Color online) Average transfer efficiency  $\eta$ , computed starting from the subradiant state  $|SUB\rangle$  for the optimal disorder (in absence of dephasing noise)  $W_{\text{opt}} = \sqrt{2} \text{ cm}^{-1}$ , plotted as a function of the subradiant-RC detuning  $\delta E_{\text{rc}}$  (uniform grid with 100 points) for different values of the dephasing strength  $\gamma_\phi$ , as indicated in the legend. The values of the parameters are  $\Delta = 0 \text{ cm}^{-1}$ ,  $V_{\text{rc}} = 1 \text{ cm}^{-1}$ ,  $\kappa = 0.01 \text{ cm}^{-1}$ , and  $\Gamma_{\text{fl}} = 10^{-4} \text{ cm}^{-1}$ , the same as in Fig. 2. The ensemble average is over 2000 realizations of disorder.

### A. The zero-gap case

When considering the case with  $\Delta = 0$ , simple symmetry considerations show that the optimal detuning must remain  $\delta E_{\text{rc}}^{\text{opt}} = 0$  also in the presence of dephasing. In order to confirm this, we fix  $W = W_{\text{opt}}$  (see (12)) and study the efficiency as a function of the detuning  $\delta E_{\text{rc}}$  for different values of the dephasing strength  $\gamma_\phi$ .

The results are reported in Fig. 6. First of all, we observe that the presence of dephasing makes the system more and more resistant to detuning between the initial state and the RC. Indeed, while the efficiency is still maximized for  $\delta E_{\text{rc}} = 0$ , it remains high in a region which grows with  $\gamma_\phi$ . This is consistent with the fact that, while the width of the resonant peak in the variable  $\delta E_{\text{rc}}$  for  $\gamma_\phi = 0$  can be considered as an effect of quantum coherence, the incoherent dynamics generated by the Haken–Strobl master equation gives rise to higher efficiency even off-resonance.

In order to show how the optimal disorder is affected by dephasing, we fix  $\delta E_{\text{rc}} = \delta E_{\text{rc}}^{\text{opt}} = 0$  (optimal detuning in absence of dephasing) and plot the correspondent efficiency as a function of the static disorder  $W' = W/\sqrt{2}$  for different values of the dephasing  $\gamma_\phi$ , see Fig. 7. The dephasing, when not too strong compared with the fluorescence width, does not change the position of the maximal efficiency at  $W_{\text{opt}}$ .

A remarkable effect is that dephasing (if not too strong) enhances transport for small disorder strength  $W < W_{\text{opt}}$ , while it is essentially irrelevant for  $W > W_{\text{opt}}$ . This is consistent with the noise-assisted transport picture [19, 20], which predicts that the efficiency is generally enhanced by dephasing, but it also suggests that

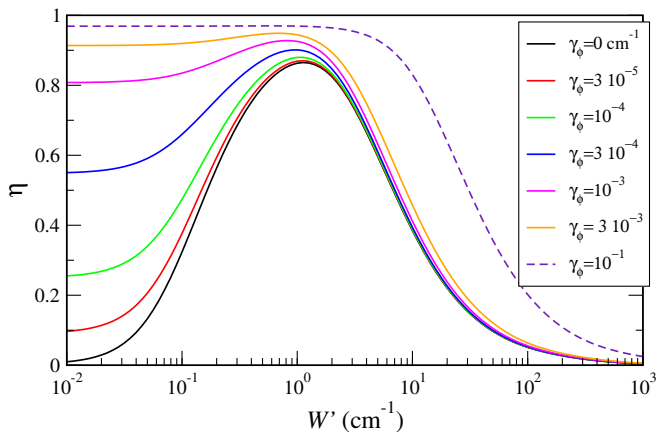


FIG. 7. (Color online) Average transfer efficiency  $\eta$ , computed starting from the subradiant state  $|SUB\rangle$  at resonance with the RC ( $\delta E_{rc} = 0$ , which is the optimal detuning in absence of dephasing) plotted as a function of the rescaled disorder strength  $W' = W/\sqrt{2}$  (uniform grid with 100 points) for different values of the dephasing strength (see legend). The values of the parameters are  $\Delta = 0 \text{ cm}^{-1}$ ,  $V_{rc} = 1 \text{ cm}^{-1}$ ,  $\kappa = 0.01 \text{ cm}^{-1}$ , and  $\Gamma_R = 10^{-4} \text{ cm}^{-1}$ , the same as in Fig. 2. The ensemble average is over 2000 realizations of disorder.

such noise-assisted transport is more efficient when the energy levels are sufficiently close to each other. For sufficiently large dephasing strength, the efficiency becomes a decreasing function of  $W'$ , in such condition static disorder is only detrimental to transport (see dashed curve in Fig. 7).

### B. The finite-gap case

The results of the previous section show that, for the zero-gap case, the presence of dephasing does not affect the estimate for the optimal detuning and also the optimal disorder is modified only for a quite large dephasing strength.

On the contrary, in the presence of a non-vanishing gap  $\Delta$  between the subradiant initial state and the superradiant one, dephasing changes the situation in a remarkable way. In Fig. 8 the average efficiency in the plane  $(W', \delta E_{rc})$  is shown for two different values of the dephasing strength. The system parameters used in this figure coincide with those of Fig. 5, except for the dephasing. In panel (a) we present the case of small dephasing  $\gamma_\phi = 10^{-4} \text{ cm}^{-1}$ : the optimal conditions are very close to the case of no dephasing (Fig. 5). Indeed, the blue dot, which represents the optimal conditions without dephasing, lies between the curves enclosing the regions of 1% and 5% below the maximal efficiency, and the small-disorder resonance condition (13) is perfectly reproduced.

On the other side, in panel (b) of Fig. 8, where the case of a larger dephasing is shown ( $\gamma_\phi = 1.26 \cdot 10^{-3} \text{ cm}^{-1}$ ), the picture is radically different. A second important resonance at  $\delta E_{rc} = \Delta$  appears (indicated by a dashed

horizontal white line). This resonance, absent for small dephasing, corresponds to the RC energy being equal to the energy of the superradiant state. Even if our previous estimate of optimal disorder still lies between the curves enclosing the regions of 1% and 5% below the maximal efficiency (blue circle in panel (b) of Fig. 8), the structure of the contour lines is very different for two reasons: (i) transport is strongly enhanced by dephasing for small disorder; (ii) due to the additional broad resonance at  $\delta E_{rc} = \Delta$ , we have two resonance peaks instead of one (compare panels (a) and (b) of Fig. 8). For a larger dephasing noise, only the broad resonance at  $\delta E_{rc} = \Delta$  remains.

We can thus conclude that the resonance  $\delta E_{rc} = V_{rc}^2/\Delta$ , given by (11), coexists, in the presence of small dephasing, with another resonance at  $\delta E_{rc} = \Delta$ , which eventually dominates the dynamics for large dephasing. The latter condition shows that, even if we start from the subradiant state, the incoherent dynamics generated by dephasing rests upon the direct transfer to the RC from the superradiant state, since the latter is continuously populated by the action of dephasing. This is at variance with the coherent resonance conditions found in the previous section.

## IV. CONCLUSIONS

We considered a paradigmatic model of quantum network, namely a trimer in which two sites are coupled to a third site, representing a reaction center where the excitation can be trapped. The optimal conditions of energy transfer are analyzed in presence of different kind of disturbances: static disorder and dynamical noise. In similar networks the states can be classified as superradiant or subradiant, based on how they transfer the excitation into the reaction center.

Subradiant states are not directly coupled to the reaction center, but static on-site disorder can effectively couple them with superradiant states. This opens an indirect path for the transfer of excitation from subradiant states to the reaction center, mediated by the superradiant state. The static disorder which activates the transfer from subradiant states, when too strong, hinders transport, so that an optimal disorder condition can be determined.

We analyze in detail such a model. Four parameters determine the different regimes in which the trimer can operate: the energy distance  $\Delta$  between the subradiant and the superradiant state, the intensity  $W$  of static disorder, which induces a random coupling between subradiant and superradiant states, the direct coupling  $V_{rc}$  between the superradiant state and the reaction center, and the detuning  $\delta E_{rc}$  between the subradiant initial state and the reaction center.

We study how to optimize the energy transfer efficiency by varying both the disorder strength  $W$  and the detuning  $\delta E_{rc}$ . The optimal conditions in absence of dephasing



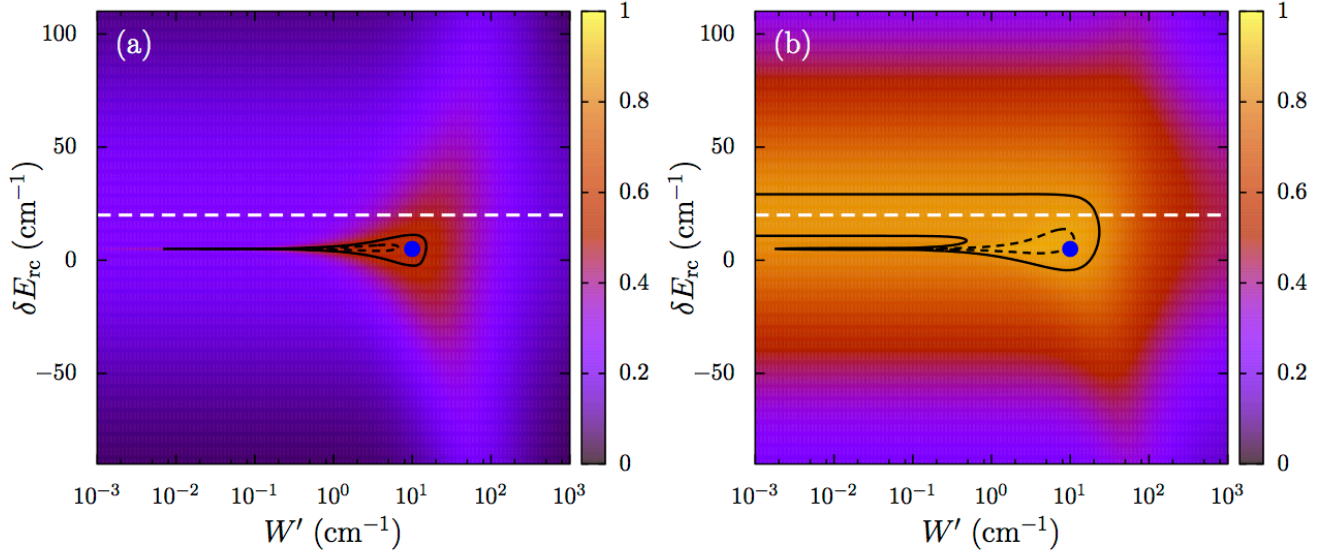


FIG. 8. (Color online) Average transfer efficiency  $\eta$ , computed starting from the subradiant state  $|SUB\rangle$ , plotted as a function of the subradiant-RC detuning  $\delta E_{rc}$  and of the rescaled disorder strength  $W' = W/\sqrt{2}$ . In panel (a) the case of small dephasing  $\gamma_\phi = 10^{-4} \text{ cm}^{-1}$  is shown and it should be compared with the results shown in Fig. 5. In panel (b) the case of larger dephasing  $\gamma_\phi = 1.26 \cdot 10^{-3} \text{ cm}^{-1}$  is shown. The blue dot indicates the estimate (13) for the optimal transfer conditions, while the horizontal dashed white line represents the condition  $\delta E_{rc} = \Delta$ . Isolines enclose the regions of efficiency lying within 1% (dashed curve) and 5% (full curve) of the maximal efficiency. The values of the parameters are  $\Delta = 20 \text{ cm}^{-1}$ ,  $V_{rc} = 10 \text{ cm}^{-1}$ ,  $\kappa = 0.01 \text{ cm}^{-1}$ , and  $\Gamma_{fl} = 10^{-4} \text{ cm}^{-1}$ , the same as in Fig. 5. We sampled the efficiency on a  $120 \times 400$  uniform grid. The ensemble average is over 2000 realizations of static disorder.

noise are given by:

- (i)  $W \simeq V_{rc}$  and  $\delta E_{rc} = 0$  for  $V_{rc} \gg \Delta$ ;
- (ii)  $W \simeq V_{rc}$  and  $\delta E_{rc} = V_{rc}^2/\Delta$  for  $V_{rc} \lesssim \Delta$ .

The origin of conditions (i) and (ii) can be synthetically expressed as follows. The disorder strength  $W$  determines the amplitude of the coupling between the subradiant donor state (D) and the superradiant bridge state (B), while  $V_{rc}$  is the coupling between the superradiant bridge state (B) and the RC acceptor state (A). Thus the condition  $W \simeq V_{rc}$  implies a symmetry between the D-B and B-A couplings, which optimizes transport. Moreover, the condition  $\delta E_{rc} = 0$  corresponds to a donor and an acceptor with the same energy, which also helps transport in a coherent regime. On the other hand, when  $W \simeq V_{rc} \lesssim \Delta$ , the stochastic nature of the D-B coupling induces a shift of the optimal detuning, which is now determined by the presence, for small values of the D-B coupling, of a sharp resonance in the transfer efficiency at  $\delta E_{rc} = V_{rc}^2/\Delta$ .

Regarding the effect of dynamical noise (modeled as pure dephasing) on the various coherent features we analyze, we show that our condition for the optimal disorder is still valid for a not too strong dephasing. On the other hand, the optimal detuning can be strongly modified, since dephasing produces an additional resonance peak, corresponding to the superradiant bridge energy being equal to that of the RC acceptor. Such peak coexists

with the one obtained via the coherent resonance conditions given above. Dephasing produces a general enhancement of the transfer efficiency for small disorder, providing also a significant stability with respect to the energy detuning  $\delta E_{rc}$ .

We believe that the principles of our analysis, even if it has been carried out on a very simple model, are relevant to all those quantum networks in which a subradiant (or trapping-free) subspace is present. Specifically, we think that the interplay of an incoherent resonant condition with a coherent one is a generic feature of those quantum networks aimed at modeling realistic light-harvesting complexes, such as ring structures with a trapping site at their center akin to those observed in natural LHI complexes.

Especially to understand the enhancement in transport due to disorder, which is ubiquitous in natural light-harvesting complexes, it is necessary to go beyond the standard perturbative analysis, since the coupling between peripheral sites and the reaction center is coherently enhanced by superradiance, producing a nontrivial interplay with the various sources of noise and disorder.

## ACKNOWLEDGMENTS

The authors acknowledge useful discussions with Lev Kaplan, Debora Contreras-Pulido, and Robin Kaiser. G.G. gratefully acknowledges the support of the Math-

- 
- [1] G. S. Engel, T. R. Calhoun, E. L. Read, T. K. Ahn, T. Mancal, Y. C. Cheng, R. E. Blankenship and G. R. Fleming, *Nature* **446**, 782 - 786 (2007); G. Panitchayangkoon, D. Hayes, K. A. Fransted, J. R. Caram, E. Harel, J. Z. Wen, R. E. Blankenship and G. S. Engel, *Proc. Nat. Acad. Sci. Am.* **107**, 12766–12770, (2010); E. Collini, C. Wong, K. Wilk, P. Curmi, P. Brumer and G. Scholes, *Nature* **463**, 644–649, (2010).
- [2] G. L. Celardo, F. Borgonovi, V. I. Tsifrinovich, M. Merkli and G. P. Berman, *J. Phys. Chem. C* **116**, 22105 (2012).
- [3] D. Ferrari, G. L. Celardo, G. P. Berman, R. T. Sayre, and F. Borgonovi, *J. Phys. Chem. C* **118**, 20 (2014).
- [4] S. Lloyd and M. Mohseni, *New J. Phys.* **12**, 075020 (2010); G. D. Scholes, *Chem. Phys.* **275**, 373 (2002).
- [5] P. W. Anderson, *Phys. Rev.* **109**, 1492 (1958).
- [6] F. Caruso, A. W. Chin, A. Datta, S. F. Huelga, and M. B. Plenio, *J. Chem. Phys.* **131**, 105106 (2009).
- [7] V. V. Sokolov and V. G. Zelevinsky, *Nucl. Phys.* **A504**, 562 (1989); *Phys. Lett. B* **202**, 10 (1988); I. Rotter, *Rep. Prog. Phys.* **54**, 635 (1991); V. V. Sokolov and V. G. Zelevinsky, *Ann. Phys. (N.Y.)* **216**, 323 (1992).
- [8] A. F. Sadreev and I. Rotter, *J. Phys. A* **36**, 11413 (2003); M. Weiss, J. A. Méndez-Bermúdez, and T. Kottos, *Phys. Rev. B* **73**, 045103 (2006).
- [9] G. L. Celardo, F. M. Izrailev, V. G. Zelevinsky, and G. P. Berman, *Phys. Lett. B* **659**, 170 (2008); G. L. Celardo, F. M. Izrailev, V. G. Zelevinsky, and G. P. Berman, *Phys. Rev. E*, **76**, 031119 (2007).
- [10] J. Grad, G. Hernandez, and S. Mukamel, *Phys. Rev. A* **37**, 3835 (1988); F. C. Spano, J. R. Kuklinski, and S. Mukamel, *J. Chem. Phys.* **94**, 7534 (1991).
- [11] E. Akkermans, A. Gero, and R. Kaiser, *Phys. Rev. Lett.* **101**, 103602 (2008); R. Kaiser, *J. Mod. Opt.* **56**, 2082 (2009); T. Bienaime, N. Piovella, and R. Kaiser, *Phys. Rev. Lett.* **108**, 123602 (2012); E. Akkermans and A. Gero, *Euro Phys. Lett.* **101**, 54003 (2013); R. Kaiser, *Nature Physics* **8**, 363 (2012).
- [12] R. Monshouwer, M. Abrahamsson, F. van Mourik, and R. van Grondelle, *J. Phys. Chem. B* **101**, 7241 (1997).
- [13] G. L. Celardo and L. Kaplan, *Phys. Rev. B* **79**, 155108 (2009); G. L. Celardo, A. M. Smith, S. Sorathia, V. G. Zelevinsky, R. A. Senkov, and L. Kaplan, *Phys. Rev. B* **82**, 165437 (2010).
- [14] G. L. Celardo, A. Biella, L. Kaplan, and F. Borgonovi, *Fortschr. Phys.* **61**, 250–260 (2013); A. Biella, F. Borgonovi, R. Kaiser, and G. L. Celardo, *Europhys. Lett.* **103**, 57009 (2013).
- [15] G. L. Celardo, G. G. Giusteri and F. Borgonovi, *Phys. Rev. B* **90**, 075113 (2014).
- [16] G. L. Celardo, P. Poli, L. Lussardi, and F. Borgonovi, *Phys. Rev. B* **90**, 085142 (2014).
- [17] M. O. Scully and A. A. Svidzinsky, *Science* **328**, 1239 (2010).
- [18] J. S. Cao and R. J. Silbey, *J. Phys. Chem. A* **113**, 13825 (2009).
- [19] M. Mohseni, P. Rebentrost, S. Lloyd, and A. Aspuru-Guzik, *J. Chem. Phys.* **129**, 174106 (2008).
- [20] M. B. Plenio and S. F. Huelga, *New J. Phys.* **10**, 113019 (2008).
- [21] J. M. Moix, M. Khasin, and J. S. Cao, *New J. Phys.* **15**, 085010, (2013).
- [22] M. K. Sener and K. Schulten, *Phys. Rev. E* **65**, 031916 (2002); S. E. Dempster, S. Jang, and Robert J. Silbey, *J. Chem. Phys.* **114**, 10015 (2001); M. K. Sener, D. Lu, T. Ritz, S. Park, P. Fromme, and K. Schulten, *J. Phys. Chem. B* **106**, 7948–7960 (2002); K. M. Pelzer, G. B. Griffin, S. K. Gray, and G. S. Engel, *J. Chem. Phys.* **136**, 164508 (2012); J. M. Moix, Y. Zhao, and J. S. Cao, *Phys. Rev. B* **85**, 115412, (2012).
- [23] A. Olaya-Castro, C. F. Lee, F. Fassioli Olsen, and N. F. Johnson, *Phys. Rev. B* **78**, 085115 (2008).
- [24] K. Gaab and C. Bardeen, *J. Chem. Phys.* **121**, 7813 (2004).
- [25] S. M. Vlamings, V. A. Malyshev, and J. Knoester, *J. Chem. Phys.* **127**, 154719 (2007).
- [26] P. Rebentrost, M. Mohseni, I. Kassal, S. Lloyd, and A. Aspuru-Guzik, *New J. Phys.* **11**, 033003 (2009).
- [27] J. L. Wu, F. Liu, Y. Shen, J. S. Cao, and R. J. Silbey, *New J. Phys.* **12**, 105012 (2010).
- [28] A. W. Chin, A. Datta, F. Caruso, S. F. Huelga, and M. B. Plenio, *New J. Phys.* **12**, 065002 (2010).
- [29] A. W. Chin, S. F. Huelga, and M. B. Plenio, *Phil. Trans. R. Soc. A*, **370**, 3638, (2012).
- [30] J. Wu, R. J. Silbey, and J. S. Cao, *Phys. Rev. Lett.* **110**, 200402 (2013).
- [31] S. Jang, T. C. Berkelbach, and D. R. Reichman, *New J. Phys.* **15**, 105020 (2013).
- [32] X. Hu, T. Ritz, A. Damjanović, and K. Schulten, *J. Phys. Chem. B* **101**, 3854 (1997).
- [33] H. Haken and G. Strobl, *Z. Phys.* **262**, 135 (1973).
- [34] V. May and O. Kuhn, *Charge and Energy Transfer Dynamics in Molecular Systems*, Wiley-VCH, Weinheim (2004).
- [35] J. A. Leegwater, *J. Phys. Chem.* **100**, 14403 (1996).